Numerical Simulation of Tsunamis

CHARLES L. MADER[1]

Joint Tsunami Research Effort, NOAA, Hawaii Institute of Geophysics, University of Hawaii, Honolulu

(Manuscript received 28 May 1973, in revised form 20 August 1973)

ABSTRACT

Two-dimensional, time-dependent, nonlinear, incompressible, viscous flow calculations of realistic models of tsunami waves interacting with continental slopes and shelves were performed. Wave heights were observed to grow by a factor of 4 as they shoaled up a 1:15 continental slope. The second or third wave often exhibited the largest wave run-up. Comparisons with shallow water, long-wave calculations showed similar results except for short wavelength tsunamis. The damping action of submerged barriers on tsunami waves was investigated. Significant amounts of the energy of a tsunami may be reflected by submerged barriers. The numerical simulation of tsunami waves can provide realistic descriptions of their flow.

1. Introduction

The objectives of this study were to determine whether time-dependent, nonlinear, viscous calculations of an incompressible fluid could be performed for gravity waves with the extreme height to width ratios ($\sim$1/100,000) of tsunami waves and to determine if the growth of the waves could be followed as they interact with the continental slope.

The SMAC (Simplified Marker and Cell) method of Harlow and Amsden (1970) was chosen, and additional features were added to the ZUNI code—including surface particles, as described by Nichols and Hirt (1971), and a partial cell boundary condition permitting boundaries to be placed across cell diagonals.

The ZUNI code was adapted for use with the University of Hawaii IBM 360 model 65 computer, and calculations were performed of waves that resemble tsunami waves. Street *et al.* (1969) used the MAC technique to numerically simulate long water waves and found that they could numerically reproduce the observed propagation of solitary waves in a horizontal channel and the run-up of a solitary wave on a vertical wall. Street *et al.*'s work did not consider waves of the height-to-width ratios of tsunamis waves. Similar calculations were performed using the ZUNI code, and the vertical wall run-up results agreed with the experimental and numerical results of Street *et al.*

Recent calculations reported by Garcia (1972) used the arbitrary boundary marker and cell technique to study tsunamis in the vicinity of their source. The method was applied to the Mendocino Escarpment for hypothetical ocean floor displacements of 10 m in a few seconds to a minute that might result from a major earthquake on the San Andreas fault. The wave was followed numerically for the first 200 sec. A single hump was first generated which split into two crests moving in opposite directions at a speed slightly less than shallow water wave speed. The waves were slightly dispersive and had a crest elevation above mean water level of about 1 m and a period of about 1.5 min. The period of major tsunamis measured in the Pacific Ocean is generally from 10 to 30 min. The periods are estimated from tide gage records assuming that the period remains nearly constant during the shoaling of the wave from the deep ocean. The wave height of major tsunamis is generally given as 1 ± 0.5 m and is estimated from the tide gage records assuming various approximate models for the wave height growth and extrapolating back to the deep ocean.

Present evidence suggests that tsunami waves consist of a train of several large, approximately sinusoidal waves of about 1 m in height moving in the deep ocean at approximately the shallow water speed of $(gD)^{\frac{1}{2}}$ or 210 m sec^{-1} at the average Pacific Ocean depth of 4500 m, having periods of 10–30 min, wavelengths of 200–600 km, and numerous smaller waves. It is the first four or five large waves that are of primary interest.

The numerical simulation of waves that have profiles similar to those suggested by experimental evidence and the realistic simulation of the interaction of tsunami waves with the continental slope were the initial objectives of this study.

2. The numerical model

The Marker and Cell (MAC) method of Harlow and Welch (1965) is a numerical technique for calculation of viscous, incompressible flow with a free surface.

The method uses a finite-difference technique for solving the time-dependent Navier-Stokes equations.

[1] Present affiliation: Los Alamos Scientific Laboratory, Los Alamos, N.M.

These equations for two-dimensional flows are

$$\frac{\partial u}{\partial x}+\frac{\partial v}{\partial y}=0,$$

$$\frac{\partial u}{\partial t}+\frac{\partial u^2}{\partial x}+\frac{\partial uv}{\partial y}=-\frac{\partial \varphi}{\partial x}+g_x+\nu\left(\frac{\partial^2 u}{\partial x^2}+\frac{\partial^2 u}{\partial y^2}\right),$$

$$\frac{\partial v}{\partial t}+\frac{\partial uv}{\partial x}+\frac{\partial v^2}{\partial y}=-\frac{\partial \varphi}{\partial y}+g_y+\nu\left(\frac{\partial^2 v}{\partial x^2}+\frac{\partial^2 v}{\partial y^2}\right),$$

where u and v are velocity components in the x and y directions, t is time, φ is the ratio of pressure to constant density, g_x and g_y are the x and y components of body acceleration, and ν is the kinematic viscosity coefficient. The MAC method is based on an Eulerian network of rectangular cells, with velocities centered at cell boundaries and the pressure cell-centered. Just as the differential equations of motion are statements of the conservation of mass and momentum, the MAC finite-difference equations express these conservation principles for each cell, or combination of cells, in the computing mesh.

After the introduction of MAC, much attention was given to devising more accurate treatments of the free surface boundary conditions. Hirt and Shannon (1968) incorporated improved surface approximations to the normal stress conditions, and showed the necessity for satisfying the tangential stress conditions. Chan and Street (1970) developed a technique for more accurate delineation of the free surface. This permitted the free surface pressure to be specified at the surface itself, rather than at the center of the surface cell. Nichols and Hirt (1971) modified the Chan and Street procedure, devising a technique for defining the fluid surface by a set of surface marker particles that move with local fluid velocity. These particles allow surface-cell pressures in MAC to be accurately specified by means of linear interpolation or extrapolation between the known values of pressure in the nearest full cell and the desired fluid surface.

A Simplified MAC (SMAC) has been described by Harlow and Amsden (1970) which does not require the pressure to be calculated. It is possible to use the actual pressures or any initial pseudo-pressure (for internal cells) such as zero.

The computing program used for the tsunami calculations is called ZUNI and is described by Amsden (1973). The SMAC technique of Harlow and Amsden has been modified to include the Nichols and Hirt free surface treatment. A partial-cell treatment that allows a rigid free-slip obstacle to be placed through cell diagonals has also been included. The desired boundary slope is obtained by choosing the appropriate aspect ratio for the cells of the mesh. Thus, the numerical technique can be used to calculate wave run-up on exposed beaches in addition to submerged beaches.

Most of the calculations were performed with 15 cells in the Y direction and 68 cells in the X direction. The cells were rectangles 450 m high (ΔY) in Y direction and 6750 m long (ΔX) in X direction. The cell aspect ratio was 1/15. The time increment used was 3 sec. The convergence criteria used was 0.02. The water level was placed at 4550 m, or 50 m up into the eleventh cell. The gravity constant was -9.8 m sec^{-2}. The viscosity coefficient used was 2.0 gm sec^{-1} m^{-1} (0.02 poise), a value representative of the actual viscosity for water. Values between 200 and 2.0 were tried, and the viscosity did not significantly affect the results. This is as expected since the actual energy dissipation due to viscosity is only 1 in 10^7 for a viscosity of 200.

The stability requirements for the SMAC type of calculation are discussed by Welch *et al.* (1965). Since the wave front must not pass through more than one cell in one time step, we have the stability criterion

$$C\Delta t<2(\Delta X)(\Delta Y)/(\Delta X+\Delta Y),$$

where C is wave speed, ΔX and ΔY are cell widths, and Δt is the time increment. For the tsunami calculation described previously, Δt must be less than 4 sec. We ran with 3 sec and had no evidence of instability; however, attempts to run with a time step of 9 sec always resulted in unstable numerical results which quickly turned to nonsense. While Street *et al.* (1969) report that the MAC numerical method was observed to be stable for zero viscosity, analysis by Nichols and Hirt (1971) suggests the perturbations could grow if the viscosity was not larger than about 20 and smaller than 30,000 gm sec^{-1} m^{-1}. We could not determine any difference between a viscosity of 200 and 2.0 for the tsunami calculation; so if perturbations are growing, they must be doing so at a rate smaller than the errors associated with the iteration convergence criterion.

The original ZUNI code was written for the CDC 6600 and the 7600 computers. Because of the smaller amount of significance available (unless expensive double-precision arithmetic is used) on the IBM 360 model 65 computer, it was found advantageous to use the actual hydrostatic pressure for the full cells rather than pseudo-pressures (generally zero) characteristic of the SMAC method to obtain adequate convergence of the iteration process. The convergence criteria for the SMAC iteration was defined as the maximum permitted change in pressure from hydrostatic pressure in any cell between iteration steps divided by the sum of the changes at the two iteration steps.

The University of Hawaii ZUNI code includes features for prescribing the particle velocity along the left boundary as a sinusoidal function of time:

$$U=A\sin(B\times\text{TIME}) \quad \text{and} \quad U=A[\sin(B\times\text{TIME})]^2,$$

where A for shallow water Airy waves is HC/D where H is wave height, C wave speed and D depth; and B is $2\pi/T$ where T is the period.

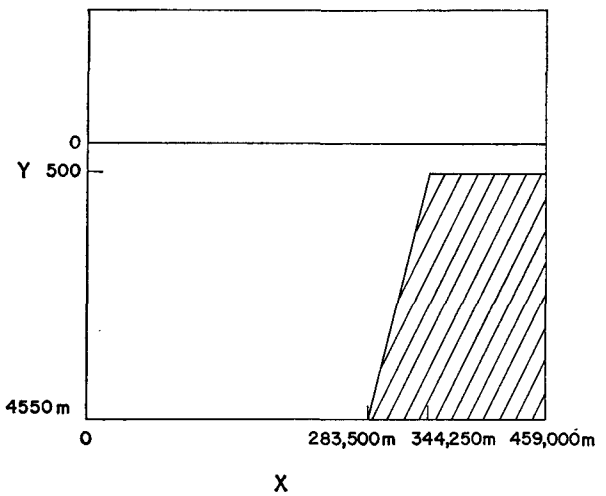

FIG. 1. A sketch of the geometry of the calculation.

The usual shallow water, long-wave theory assumes that the vertical component of motion does not influence the pressure distribution which is assumed to be hydrostatic. It is of interest to compare the results of the numerical studies solving the complete Navier-Stokes equations with those using the more conventional shallow-water, long-wave theory.

The long-wave equations are

$$\frac{\partial u}{\partial t}+u\frac{\partial u}{\partial x}+v\frac{\partial u}{\partial y}=-g\frac{\partial H}{\partial x},$$

$$\frac{\partial v}{\partial t}+u\frac{\partial v}{\partial x}+v\frac{\partial v}{\partial y}=-g\frac{\partial H}{\partial y},$$

$$\frac{\partial H}{\partial t}+\frac{\partial (D+H)u}{\partial x}+\frac{\partial (D+H)v}{\partial y}=0,$$

where u and v are velocity components in x and y direction, H is the wave height, D the water undisturbed depth and g gravity.

These equations were solved by a code called SWAN using a central difference technique where the wave height and depth were taken as cell-centered and the velocities were centered at cell boundaries. The difference equations for the SWAN code are described by Mader (1973).

3. The shoaling results

The dimensions of the shoaling calculations with a continental slope of 1:15 ending in a shelf 500 m deep are sketched in Fig. 1.

a. Solitary tsunamis

While single solitary-like waves are not realistic models of tsunami waves, they are useful for demonstrating fundamental features of the flow and for checking numerical results.

The waves were generated by prescribing as a function of time the velocity of water flowing in from the left boundary. The velocity in the X direction was prescribed as

$$U=0.04666[\sin(0.004713\times\text{TIME})]^2,$$

where TIME is in seconds. In 4550 m deep water this results in a single wave above the surface with a height of ~1 m, a width of ~140 km, a shallow water speed of 210 m sec^{-1}, and a period of ~660 sec.

The computed wave surface profiles for the 140-km wide single wave interacting with a 1:15 continental slope, running along a 500 m deep continental shelf and reflecting off a cliff are shown in Fig. 2. In Fig. 3 the profiles are shown for multiple waves.

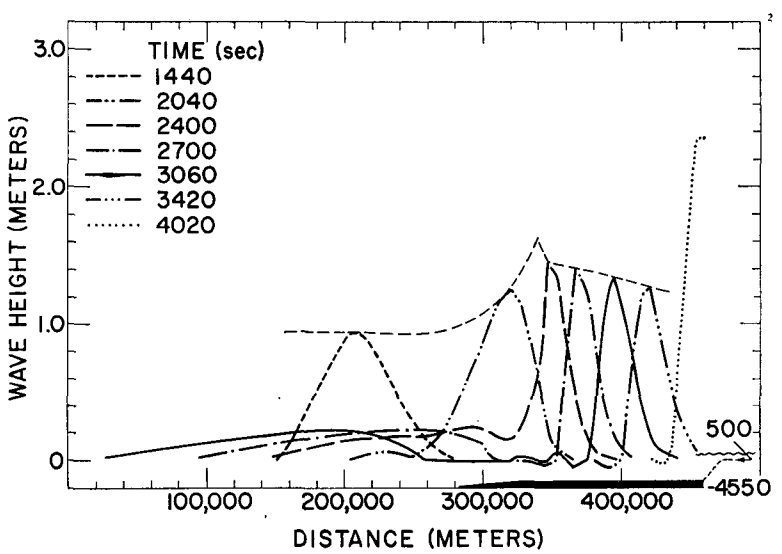

FIG. 2. Computed wave surface profiles for the 140-km wide single wave interacting with 1:15 continental slope (sketched on bottom of graph), a continental shelf 500 m deep and reflecting off a cliff.

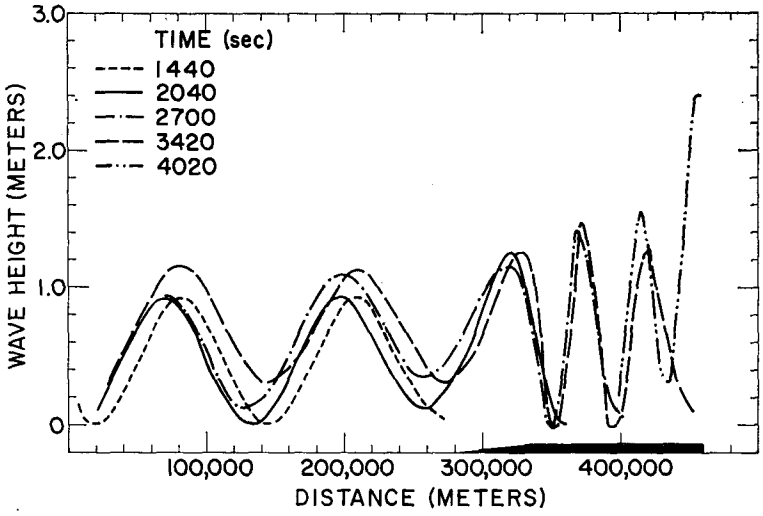

FIG. 3. Computed wave surface profiles for multiple waves at various times for for the system in Fig. 2.

As a wave proceeds up the continental slope, the wave period remains constant while the velocity decreases from approximately 210 to 70 m sec^{-1}, the wavelength decreases from approximately 140 to 47 km, the height increases from 0.95 to 1.6 m, and then slowly decreases forming a complicated train of waves. Upon reflection from the right boundary, a wave 2.4 m high is formed which is approximately double the height of the wave before it arrived at the boundary.

The experimental and numerical results for the solitary, vertical wall run-up waves of Street *et al.* (1969) show that at small values of wave height divided by depth, the slope of the wave run-up vs wave height is almost 2.0.

The computed wave surface profiles for the 140-km wide single wave running up a 1:15 continental shelf to above still water level are shown in Fig. 4. Fig. 5 shows the maximum shoaling amplitude of the wave as a function of shoaling depth. Also shown is the shallow water curve for the same example. The growth of the wave was compared with the experimental and theoretical results of Madsen and Mei (1969) for solitary waves interacting with uneven bottoms. Peregrine (1967) treated a similar problem but with less appropriate initial conditions. The results of Madsen and Mei shoal only to depths of 0.2 of the initial depth. Within this range their results are in reasonable agreement with the results shown in Figs. 2 and 3. The maximum height of the wave was 2.8 m or about three times the initial wave height of 0.95 m. This must be considered a lower limit as the resolution

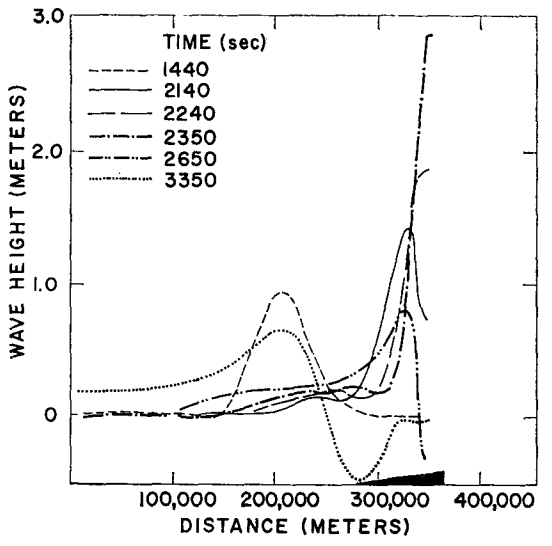

FIG. 4. Computed wave surface profiles for a single wave interacting with a 1:15 continental shelf.

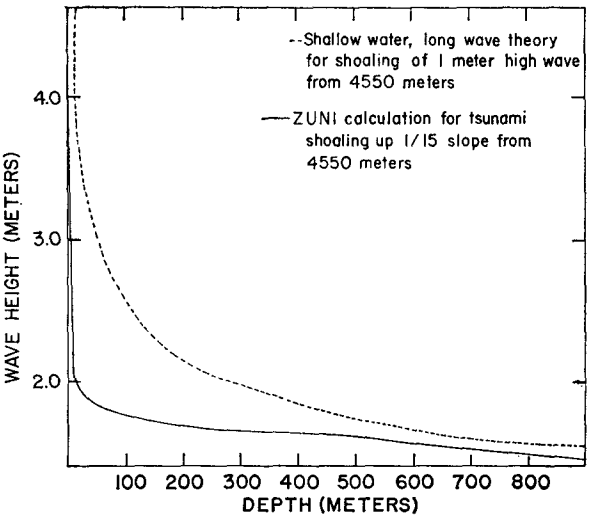

FIG. 5. The amplitude of calculated 1 m half-height, 1320-sec (or 1 m high, 660-sec single wave above surface) tsunami waves as they shoal up a 1:15 slope from 4550 m. Also shown is the shallow-water, long-wave curve.

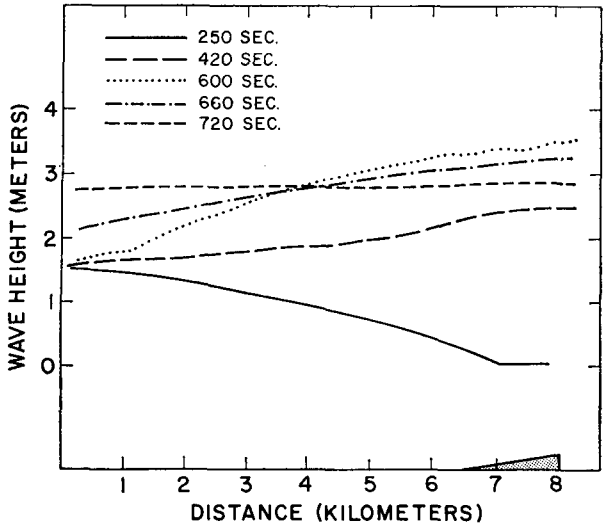

FIG. 6. Computed wave surface profiles for a 1.8 m half-height, 1320-sec tsunami shoaling up a 1:15 slope from 101.1 m.

of the calculation is inadequate to determine the maximum height.

One approach to this problem is to look only at the 100 m of water and compress the scale of the calculation by 45. As input we used a piston that would initially produce a wave of the height calculated in the previous problem at 100 m. As shown in Fig. 5, the wave height is about 1.8 m. The wave speed is closely approximated by $(gD)^{\frac{1}{2}}$ or 31.5 m sec^{-1}. For a single wave above the surface, the period is 660 sec and the wavelength 20.8 km; for a sine wave, the period is 1320 sec and the wavelength 41.6 km.

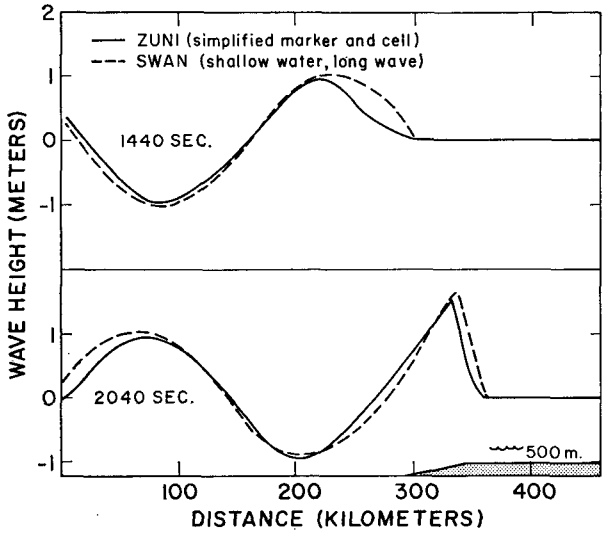

FIG. 7. Computed wave surface profiles for a 1 m half-height, 1320-sec tsunami interacting with a 1:15 continental slope, a continental shelf 500 m deep and reflecting off a cliff; and the shallow-water, long-wave calculations for the same model.

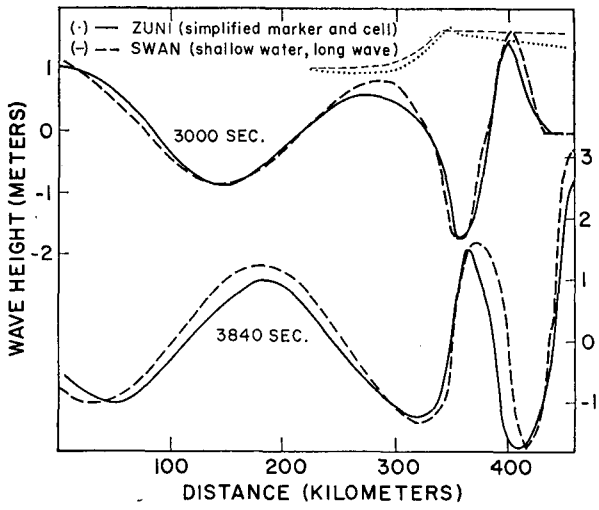

FIG. 8. Continuation of Fig. 7.

The calculation was performed with a mesh of 15×68 cells as before with a ΔX of 150, ΔY of 10, Δt of 0.5, and a convergence error of 0.002; the 1:15 slope was started at the 42nd cell or at 6300 m. The depth was 101.1 m and $U=0.567\sin[0.004713\times\text{TIME}]$. The wave profiles are shown in Fig. 6, and the maximum height of the wave is 3.47 m or about 1.9 times the 1.8 m wave height used initially in the calculation and 3.6 times the 0.95 wave height before any shoaling had occurred. The wave then flattens to a height of 2.75±0.1 m over the width considered. This is close to the 2.8 value calculated by the less resolved calculation. This also explains the flat top observed upon reflection in the less resolved calculation. It is apparently a realistic average height for the cell size used, and the flat top over several cell widths is also apparently correct.

For a more realistic model of a tsunami, we used sine waves with a half-height of 0.5 or 1 m, a period of 1320 or 660 sec, and a wavelength of 280 or 140 km.

b. One meter half-height, 1320-sec tsunamis

Using a piston velocity prescribed by

$$U=0.04666\sin(0.004713\times\text{TIME}),$$

a wave develops in 4550 m deep water of approximately 0.95 m half-height, with a wavelength of ~280 km, a period of 1320 sec, and a speed of 210 m sec^{-1}. the wave is slightly dispersive as it proceeds up a constant depth channel.

The wave surface profiles were computed for the tsunami interacting with a 1:15 continental slope, running along a 500 m deep continental shelf and reflecting off a cliff. The profiles are similar to those shown in Figs. 2 and 3. The peak shoaling height is 1.6 m which decreases to 1.4 m before it reflects off the wall with maximum and minimum heights of +2.75, −3.4, +2.75 m.

The calculated wave surface profiles are shown in Figs. 7 and 8 along with the shallow-water, long-wave calculations using the SWAN code for the identical model. The long-wave results do not disperse in the deep channel, do shoal higher and steeper, and do not disperse as they run along the shallow channel. Experimental evidence that such waves should disperse in the shallow channel is given by Madsen and Mei (1969). The wave that reflects from the wall in the SWAN calculation is 20% higher than the reflected wave in the ZUNI calculation.

Fig. 9 shows the computed wave surface profiles as the tsunami interacts with a 1:15 continental slope. The maximum and minimum calculated heights are +2.83, −4.0, +3.76, −4.11, +4.04 m. So the maximum run-up does not result from the shoaling of the first wave but from the shoaling of the second or third wave. Such behavior has been observed for real tsunamis. We can now place an upper limit of tsunami wave growth from shoaling up a 1:15 continental slope of at least 4.0. As discussed earlier and shown in Fig. 6, the scale of the calculation is such that this should be considered an average over the cell size used rather than the actual maximum values.

For a tsunami interacting with a 1:15 continental slope, running along a 950 m deep continental shelf and reflecting off a cliff, the peak shoaling height is 1.5 m which decreases to 1.32 m before it reflects off the wall with maximum and minimum heights of +2.56, −3.0, +2.48 m.

c. One meter half-height, 660-sec tsunamis

Using a piston velocity prescribed by

$$U = 0.04666 \sin(0.009426 \times \text{TIME}),$$

a wave develops in 4550 m deep water of approximately 0.86 m half-height. The shorter wavelength wave is more dispersive than the longer one discussed in Section 3b.

The wave surface profiles were computed for the tsunami interacting with a 1:15 continental slope, running along a 500 m deep continental shelf and reflecting off a cliff. The peak shoaling height is 1.4 m which decreases to 0.68 m before it reflects off the wall to a first wave maximum of 1.15 m. Subsequent wave interactions result in much larger wave run-ups.

The wave surface profiles were computed for the tsunami interacting with a 1:15 continental slope. The maximum calculated heights are +2.14, −3.56, +3.44, −3.9, +3.6 m. Again the upper limit of tsunami wave growth from shoaling is at least a factor of 4.0.

The surface wave profiles were calculated for a 1.8 m half-height, 660-sec tsunami shoaling up a 1:15 slope from 101.1 m. Comparison with the wave profiles shown in Fig. 6 shows that, with the same height at 101 m, the smaller wavelength shoals to a higher level but for a shorter distance and time.

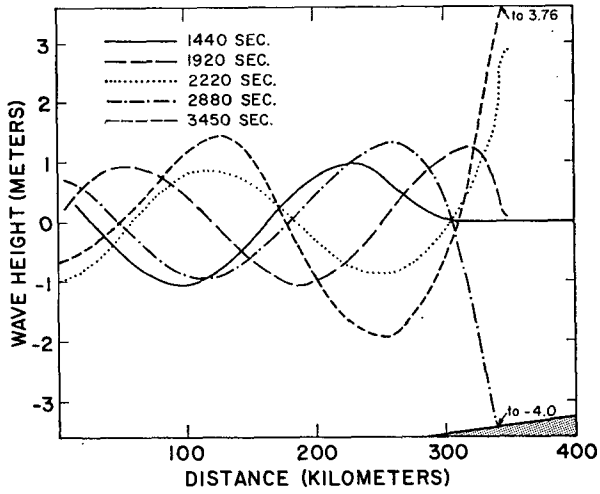

FIG. 9. Computed wave surface profiles for the wave in Fig. 7 interacting with a 1:15 continental shelf.

d. Half meter half-height, 660-sec tsunamis

Using a piston velocity prescribed by:

$$U = 0.02333 \sin(0.009426 \times \text{TIME}),$$

a wave develops in 4550 m deep water of ~0.4 m half-height.

The wave surface profiles were computed for the tsunami interacting with a 1:15 continental slope, running along a 500 m deep continental shelf and reflecting off a cliff. The peak shoaling height is 0.62 m which disperses as it runs along the shelf to 0.28 m. The wave run-up heights are +0.4, −1.32, +1.10, −2.10, +1.10, −1.72 m.

Some of the calculated wave surface profiles are shown in Fig. 10 along with the shallow-water, long-

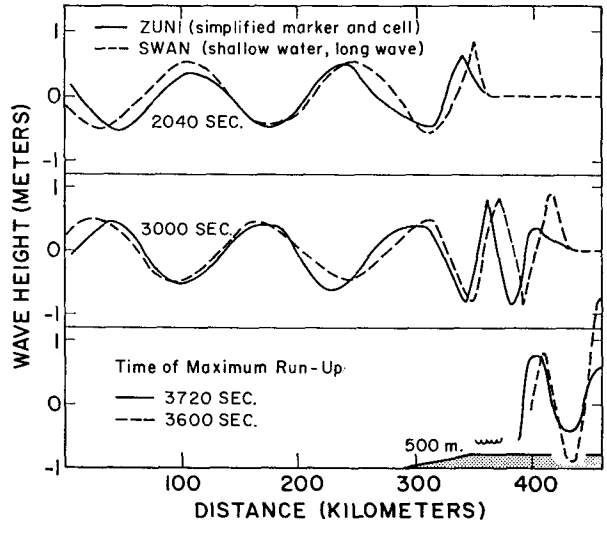

FIG. 10. Computed wave surface profiles for a 0.5 m half-height 660-sec tsunami interacting with a 1:15 continental slope, a continental shelf 500 m deep and reflecting off a cliff; and the shallow water, long-wave calculations for the same model.

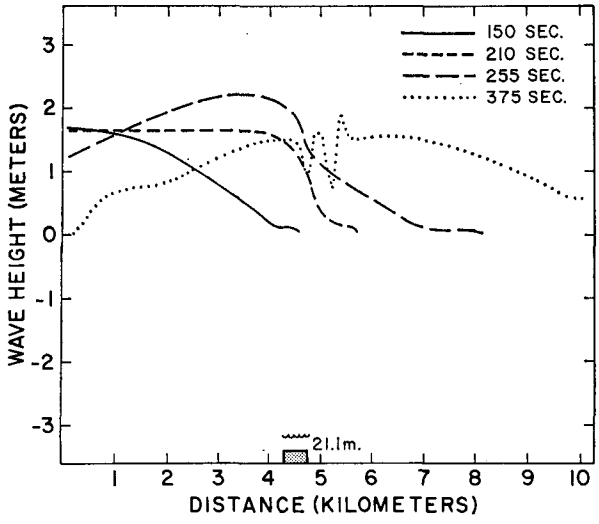

FIG. 11. Surface wave profiles for a 660-sec tsunami interacting with a 21.1 m deep barrier.

wave calculations using the SWAN code for the identical model. The difference between the two calculations increases as the wave progresses, becoming different by a factor of 2 upon reflecting from the wall. While it could be stated that this is an example where the long-wave, shallow-water assumptions lead to appreciable error, this is not necessarily true since we do not know the nature of tsunami waves well enough to determine if the tsunami should be more like the long-wave model or the one we used.

Since most tsunami waves that have been observed after travel across the ocean have periods longer than 10 min, it is tempting to postulate that this is because the shorter waves are so dispersive that they cannot propagate long distances.

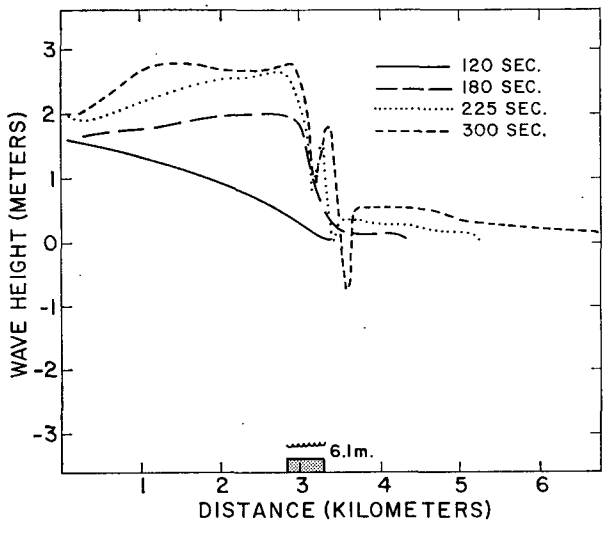

FIG. 12. Surface wave profiles for a 660-sec tsunami interacting with a 6.1 m deep barrier.

The surface wave profiles were computed as the tsunami interacts with a 1:15 continental slope. The maximum and minimum calculated are +0.91, −2.03, +1.5, −1.79, +1.68, −2.1, +1.54 m. Again, the upper limit of the tsunami wave growth from shoaling is at least a factor of 4.0.

4. The underwater barrier results

A submerged barrier usually absorbs some of the wave energy by causing the wave to break prematurely and reflecting part of the wave energy back seaward. Tsunami waves are of sufficiently long wavelength that they do not break, so underwater barriers will be effective only as reflectors of the energy. The shallow-water, long-wave theory is inadequate to describe the effect of underwater barriers on tsunami waves because the vertical component of velocity is a crucial feature of the flow.

Johnson *et al.* (1951) present results of an experimental investigation of the damping action of submerged rectangular breakwaters. They use the inshore wave height divided by the seaward wave height before interaction with the barrier as the transmission coefficient, and graph it against the dimensionless quantity of barrier height divided by channel water depth.

The calculations were performed assuming the barrier was located in 101.1 m of water and extended to within 21.1, 11.1, and 6.1 m of the still water surface. The wave height at 100 m of 1.8 m from Fig. 5 was assumed. The wave period assumed was 1320, 660, and, for a more detailed wave interaction calculation, a short period of 110 sec.

The 21.1 and 11.1 m deep barriers used the mesh described previously for Fig. 6. The barrier was 450 m wide, occupying cells 30–32 or from 4350–4800 m. The

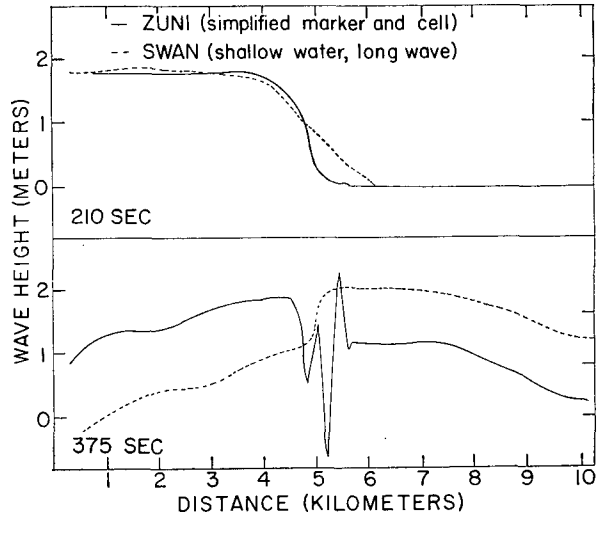

FIG. 13. Surface wave profiles for a 660-sec tsunami interacting with a 11.1 m deep barrier, and the shallow-water, long-wave profiles for the same model.

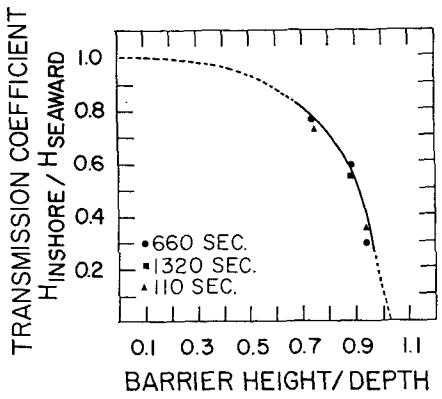

FIG. 14. The calculated transmission coefficient of tsunami waves as a function of barrier height divided by depth.

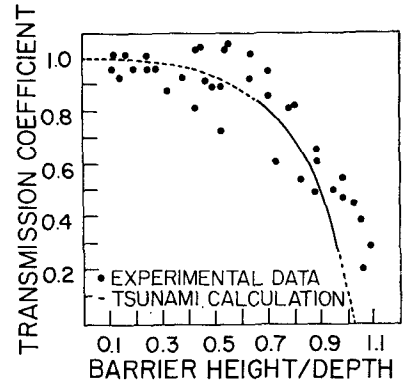

FIG. 15. The Johnson *et al.* experimental submerged breakwater data and the calculated tsunami curve in Fig. 14.

position of the barrier is shown on the bottom of the figures.

The 6.1 m deep barrier calculation was performed using a mesh of 23×45 cells with a ΔX of 150, ΔY of 5.0, Δt of 0.3, and a convergence error of 0.002; the barrier was 450 m wide, occupying cells 20–22 or from 2850–3300 m.

The surface wave profiles for a 660-sec period tsunami interacting with barriers 21.1, 6.1 and 11.1 m below the water surface are shown in Figs. 11, 12 and 13. The initial inshore wave heights are 1.4, 1.1 and 0.54 m, for the 21.1, 11.1 and 6.1 m deep barriers, respectively, for an undisturbed seaward height of 1.84 m. The 6.1 m height is so far below the seaward height that it is probably a lower limit value. The calculation was not used to later times as the wave height was being appreciably disturbed by the right boundary.

Fig. 13 also shows a comparison of the surface wave profiles for a barrier 11.1 m below the water surface with shallow-water, long-wave calculations. As expected, the long-wave model is inadequate.

The surface wave profiles were calculated for a 1320-sec period tsunami interacting with a 11.1 m deep barrier. The initial inshore wave height is 1.03 m. This is probably a lower limit since the seaward height is significantly larger at the time the calculation was ended because it was being disturbed by the right boundary.

The surface wave profiles were calculated for a 110-sec period tsunami interacting with barriers 21.1, 11.1 and 6.1 m below the water surface. The initial inshore wave heights are 1.34, 1.046 and 0.35 m, respectively, for an undisturbed seaward height of 1.9 m.

The transmission coefficient as a function of the barrier height divided by depth is shown in Fig. 14. The experimental data from Figs. 4 and 5 of Johnson *et al.* (1951) and the tsunami curve of Fig. 14 are shown in Fig. 15. While the characteristics are quite different between the experimental and calculated waves, the effectiveness of the underwater barrier appears similar.

5. Conclusions

The detailed numerical simulation of gravity waves that resemble the profile of actual tsunami waves has been achieved. Realistic simulation of the interaction of tsunami waves with slopes that resemble the continental slope has been demonstrated. Wave heights were observed to increase by a factor of 4 as they shoaled up a 1:15 continental slope. The second or third wave often exhibited the highest wave run-up.

Similar results can be obtained using shallow-water, long-wave theory for long wavelength tsunamis, but fail to be adequate for short wavelength tsunamis.

Underwater barriers can reflect significant amounts of the tsunami energy. The shallow-water, long-wave theory is inadequate to describe the flow of tsunamis over underwater barriers.

The numerical simulation of tsunami waves has been demonstrated. The extension of the SMAC numerical technique to three dimensions has already been accomplished at Los Alamos Scientific Laboratory. Three-dimensional calculations of tsunami waves interacting with harbors, with multi-dimensional barriers, and with the ocean floor over the entire ocean are within the state-of-the-art.

Acknowledgments. The author gratefully acknowledges the essential contributions to the revised ZUNI code of A. Amsden, D. Butler and F. H. Harlow of the Los Alamos Scientific Laboratory. Discussion with B. D. Nichols of Los Alamos Scientific Laboratory, C. W. Hirt and R. D. C. Chan of Science Applications, Inc., D. Stoutemyer of the University of Hawaii, and with H. G. Loomis and G. R. Miller of Joint Tsunami Research Effort have been especially valuable.

This work was performed under a National Oceanic and Atmospheric Administration Grant 04-3-022-3 by the author while on sabbatical leave from the Los

Alamos Scientific Laboratory of the University of California.

REFERENCES

Amsden, A. A., 1973: Numerical calculation of surface waves: A modified ZUNI code with surface particles and partial cells. Rept. LA-5146, Los Alamos Scientific Laboratory.

Chan, R. K. C., and R. L. Street, 1970: A computer study of finite-amplitude water waves. *J. Comput. Phys.*, **6**, 68–94.

Garcia, W. J., 1972: A study of water waves generated by tectonic displacements. Rept. HEL 16-9, College of Engineering, University of California at Berkeley.

Harlow, F. H., and A. A. Amsden, 1970: A simplified MAC technique for incompressible fluid flow calculations. *J. Comput. Phys.*, **6**, 322–325.

—— and J. E. Welch, 1965: Numerical study of large amplitude free surface motions. *Phys. Fluids*, **9**, 842–851.

Hirt, C. W., and J. P. Shannon, 1968: Free surface stress conditions for incompressible flow calculations. *J. Comput. Phys.*, **2**, 403–411.

Johnson, J. W., R. A. Fuchs and J. R. Morison, 1951: The damping action of submerged breakwaters. *Trans. Amer. Geophys. Union*, **32**, 704–718.

Mader, C. L., 1973: Numerical simulation of tsunamis. Rept. HIG-73-3, Hawaii Institute of Geophysics, University of Hawaii.

Madsen, O. S., and C. C. Mei, 1969: Transformation of a solitary wave over an uneven bottom. *J. Fluid Mech.*, **39**, 781–791.

Nichols, B. D., and C. W. Hirt, 1971: Improved free surface boundary conditions for numerical incompressible-flow calculations. *J. Comput. Phys.*, **8**, 434–448.

Peregrine, D. H., 1967: Long waves on a beach. *J. Fluid Mech.*, **27**, 815–827.

Street, R. L., R. K. C. Chan and J. E. Fromm, 1969: The numerical simulation of long water waves-progress on two fronts. *Tsunamis in the Pacific Ocean*, W. M. Adams, Ed., Honolulu, East-West Center Press, 453–473.

Welch, J. E., F. H. Harlow, J. P. Shannon and B. J. Daly, 1965: The MAC method: A computing technique for solving viscous, incompressible, transient fluid-flow problems involving free surfaces. Rept. LA-3425, Los Alamos Scientific Laboratory.